



## Assessment of different ceramic filtration membranes as a separator in microbial fuel cells

Euntae Yang<sup>a</sup>, Kyu-Jung Chae<sup>b</sup>, In S. Kim<sup>a,\*</sup>

<sup>a</sup>Global Desalination Research Center (GDRC), School of Environmental Science and Engineering, Gwangju Institute of Science and Technology (GIST), 123 Cheomdan-gwagiro, Buk-gu, Gwangju 61005, South Korea, email: [iskim@gist.ac.kr](mailto:iskim@gist.ac.kr) (I.S. Kim)

<sup>b</sup>Department of Environmental Engineering, Korea Maritime and Ocean University, 727 Taejong-ro, Yeongdo-Gu, Busan 49112, South Korea

Received 16 February 2016; Accepted 22 April 2016

### ABSTRACT

Membranes damaged by irreversible fouling and microbial and chemical attacks need to be replaced, significantly increasing the operational and maintenance costs of microbial fuel cells (MFCs) in field applications. Here, two different ceramic filtration membranes (Anodisc 13 and Sterlitech 15), which have long lifespans due to their strong mechanical strength, chemical stability, and relatively low fouling propensities, were employed in a two-chamber MFC, and compared to Nafion 117. Anodisc 13 showed a similar electrical membrane resistance (3.0  $\Omega$ ) to Nafion 117 (1.7  $\Omega$ ), whereas Sterlitech 15 had a significantly higher electrical membrane resistance (226  $\Omega$ ). Higher oxygen and substrate transport coefficients ( $6.30 \times 10^{-4}$  and  $23.2 \times 10^{-7}$ ) were obtained with Anodisc 13, but lower ( $0.08 \times 10^{-4}$  and  $1.30 \times 10^{-7}$ ) were observed with Sterlitech 15, compared to Nafion 117 ( $3.60 \times 10^{-4}$  and  $9.50 \times 10^{-7}$ ). However, during MFC operation, the highest voltage ( $67.7 \pm 1.9$  mV) was generated when using Anodisc 13, followed by Nafion 117 ( $57.3 \pm 3.6$  mV) and Sterlitech 15 ( $32.9 \pm 1.8$  mV), due to the facilitated ion transport arising from the large pore size (0.1  $\mu\text{m}$ ), smaller thickness (67  $\mu\text{m}$ ), and highly porous and non-tortuous pore structure of Anodisc 13.

*Keywords:* Bioelectrochemical system; Ceramic filtration membrane; Microbial fuel cell; Separator

### 1. Introduction

The use of microbial fuel cells (MFCs) has benefits in treating wastewater as they can simultaneously recover electricity from organic matter [1]. A typical MFC configuration consists of an anaerobic anode chamber containing electrochemically active bacteria (EAB) for substrate oxidation and an aerobic cathode chamber for oxygen reduction. The environments in

these two chambers are remarkably different; as such, they need to be physically partitioned. In contrast, protons, released by EAB, freely transport from the anode to cathode chambers as electrons transfer in order to maintain the charge balance.

The most common separators in MFCs are proton exchange membranes (PEMs; e.g. Nafion) because of their high proton conductivity [2–4]. However, challenges related to the installation of PEMs (e.g. poor proton transfer, unfavorable oxygen diffusion, biofouling, and expense) have impeded the forward

\*Corresponding author.

movement of MFC technologies for practical applications [2–6]. First, the proton diffusion capability of PEMs severely degenerates by the preoccupation of negatively charged functional groups in PEMs by other abundant cations (e.g.  $\text{Na}^+$ ,  $\text{K}^+$ ,  $\text{Ca}^{2+}$ ,  $\text{Mg}^{2+}$ , and  $\text{NH}_4^+$ ) that exist in the MFC anolyte, and consequently inducing a pH gradient between the anode and cathode chambers in MFCs [6,7]. Second, the relatively high oxygen permeability of PEMs inhibits EAB metabolism in the anode, which results in a loss of electrons. Finally, PEMs can deteriorate due to fouling and chemical attacks [6,8–10].

According to Xu et al. [9], the fouling layer on PEMs increases the internal resistance of MFCs by 20% and significantly decreases their power output (by 32.3%). However, the formation of a fouling layer on PEMs is unavoidable during the long-term operation of MFCs [2,8]; physical or chemical membrane processes to clean or remove fouling is typically required when MFCs are operated at actual sites. This membrane cleaning could, however, damage the PEMs [11]; fouled PEMs ultimately need to be replaced with new PEMs, thereby increasing the capital cost of MFCs—PEMs account for approximately 40% of the capital cost of MFCs (i.e. the cost of Nafion, the most common commercial PEM, is about 1,400 US  $\$/\text{m}^2$  [4]) [12]. Therefore, there is a strong need to investigate more effective PEM alternatives prior to commercializing MFC technologies.

Recently, diverse materials such as ion exchange membranes (IEMs), salt bridges, and porous materials have been evaluated as PEM alternatives in MFCs, based on their power density (PD) output [3,5,13–18]. Among these alternative separators, polymeric porous separators (e.g. J-cloth, ultrafiltration membranes, microfiltration membranes, and forward osmosis membranes) have generally exhibited better performance than ion exchange separators in MFCs due to their excellent proton transfer, despite their high oxygen and substrate crossover rates [4]. Moreover, polymeric porous membranes are considered relatively more cost-effective [3,4,6]. However, these water treatment membranes inevitably deteriorate due to biodegradation and fouling [13,19], such that periodic cleaning and membrane replacements remain as requirements for long-term operation.

To overcome these drawbacks, porous ceramic materials have been applied as separators in MFCs due to their high chemical and mechanical stability [3,17,20,21]. For example, Winfield et al. [17] reported that ceramic MFCs equipped with earthenware clay as a separator achieved comparable PD to PEM-based conventional MFCs during long-term operation. In another study, Winfield et al. [21] also evaluated

terracotta and earthenware for use as separators in MFCs, and found that a less ion-rich and more porous ceramic material is preferable. More recently, Pasternak et al. [20] compared the performance and cost of four different ceramic materials in MFCs (i.e. mullite, earthenware, pyrophyllite, and alumina). In both short- and long-term operations, pyrophyllite, having a wall thickness of 3 mm and a porosity of 2%, generated the highest power densities of 6.93 and 4.3  $\text{W}/\text{m}^3$ .

Through these previous studies, the applicability of porous ceramic materials for MFCs has been proven. However, the application of ceramic filtration membranes, which generally have a high porosity and uniformly sized pores, in MFCs has yet to be systematically investigated as a separator; herein, we explore ceramic micro- and ultrafiltration membranes as separators in MFCs. If ceramic filtration membranes can be successfully applied to MFCs, both electricity generation and high-quality effluent production can be achieved by taking advantage of membrane filtration in MFCs. Note that the cost of ceramic filtration membranes is generally 10 times higher than polymeric filtration membranes [22]; despite their high initial introduction costs, ceramic filtration membranes have great potential for use as separators in the practical implementation of MFC technologies. Importantly, the long operational lifetime of ceramic filtration membrane can reduce the capital cost of MFCs by lengthening the replacement cycle of membranes.

This study initially focuses on a methodical investigation of ceramic filtration membrane characteristics for use as a MFC separator by analyzing their morphology, mass transport, and electrical resistance. Actual performances (cell voltage output and maximum PD) and internal resistances of MFCs having a ceramic filtration membrane and a PEM are then compared.

## 2. Materials and methods

### 2.1. Ceramic filtration membrane characterization

Ultrafiltration membrane 15 KD (Sterlitech 15A) and microfiltration ceramic filtration membranes (Anodisc 13) were, respectively, purchased from Sterlitech Corporation (USA) and Whatman (USA) for this study. A Nafion 117 (Dupont, USA) membrane, the most popular PEM for MFC separators, was prepared as the control. The membrane structures were observed using scanning electron microscopy (SEM; S-4700, Hitachi, Japan).

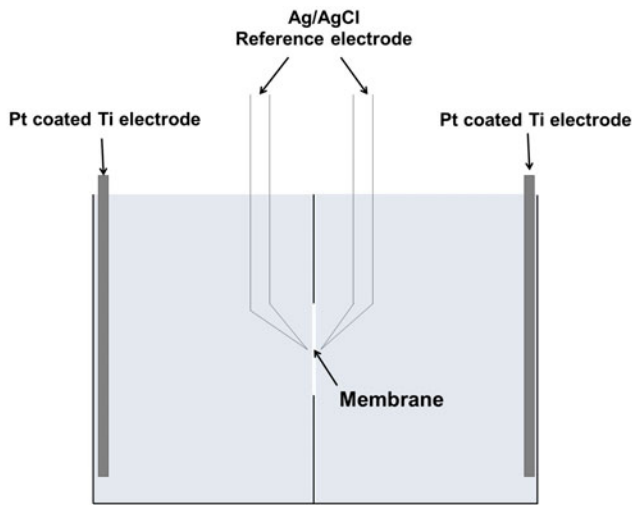


Fig. 1. Two-chambered electrochemical cell used for membrane resistance measurements.

In Fig. 1, an electrochemical cell was used to analyze the electrical resistances of the membranes. The cell consisted of two compartments, a pair of platinum-coated titanium electrodes located at both ends of the cell, and a pair of Ag/AgCl Luggin reference electrodes that were placed near both sides of the membrane being tested. A test membrane (effective area:  $0.76 \text{ cm}^2$ ) was set up between the two compartments, and both compartments were filled with 130 mL of 0.5 M NaCl solution. The impedance spectra analyses of the four-electrode electrochemical cell were subsequently analyzed using a potentiostat (Autolab PGSTAT 30, EcoChemie, The Netherlands) over a frequency range from  $10^{-1}$  to  $10^5$  Hz.

The tests of dissolved oxygen (DO) transport through the membranes were performed using abiotic MFC reactors. The anode of the abiotic MFC reactor contained an oxygen-free nutrient mineral buffer solution (NMB; 50 mM, pH 7), which was sparged with nitrogen gas for 20 min, and the cathode contained phosphate buffer solution (PBS; 50 mM, pH 7). The anode chamber was kept airtight to maintain anaerobic conditions, whereas the cathode chamber was continuously aerated to ensure DO saturation conditions during the tests. The DO concentration of the anode chamber was monitored using a DO meter (Orion Star A323, Thermo Scientific, USA), measured at 1 h intervals. The mass transfer coefficient of DO ( $K_o$ ) was determined according to [2]:

$$K_o = -v/At \ln[(C_o - C)/C_o] \quad (1)$$

where  $v$  is the anode chamber liquid volume,  $A$  is the membrane projected area,  $C_o$  is the DO concentration of the cathode chamber, and  $C$  is the DO concentration of the anode chamber at time  $t$ .

Substrate diffusion through the membranes was investigated using abiotic MFC reactors. The anode and cathode chambers were filled with sterilized NMB solution (50 mM, pH 7) containing 450 mg/L sodium acetate and PBS (50 mM, pH 7), respectively. To observe the substrate concentration changes in each chamber over time, the solutions in each chamber were collected every 4 h, and the substrate concentration in the samples was then analyzed using a total organic carbon analyzer (TOC-L, Shimadzu, Japan). The mass transfer coefficient for the substrate was calculated using the following formula [23]:

$$K_s = -v/2At \ln[(C_o - 2C_2)/C_o] \quad (2)$$

## 2.2. MFC reactor design and experimental setup

A two-chambered H-type MFC reactor was constructed (Fig. 2). The working volume of each chamber was 130 mL, and the two chambers were separated using a membrane (CEM or ceramic filtration membrane; projected area:  $0.76 \text{ cm}^2$ ). A pretreated carbon felt ( $2.5 \times 5 \text{ cm}$ , 6 mm thickness; Morgan, UK) connected to a platinum wire was installed as the anode electrode [2], and a carbon felt ( $2.5 \times 5 \text{ cm}$ , 6 mm thickness) having platinum catalysts (about  $0.5 \text{ mg/cm}^2$ ) connected to a platinum wire was used

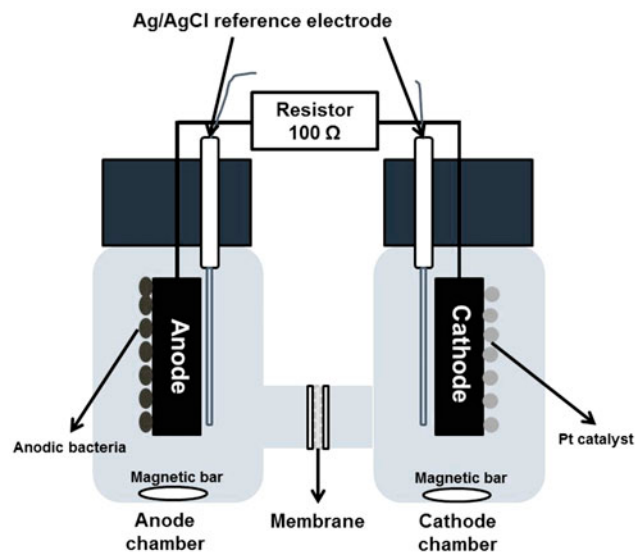


Fig. 2. Schematic of an H-type two-chambered MFC.

as the cathode electrode. To measure the potential at the electrodes, each chamber was fitted with an Ag/AgCl reference electrode (195 mV vs. SHE; Microelectrode, USA).

To inoculate the anode electrode, the anode chamber was filled with a mixture of 50 mM NMB, 0.5 mM sodium acetate, and anaerobic digestion sludge (20% v/v), which was acquired from the Gwangju Municipal Wastewater Treatment Plant in South Korea. The MFC reactor was then operated under acetate feeding and an external resistance of 100  $\Omega$  at a controlled room temperature of 25 °C for two months prior to these experiments. For the anolyte, the NMB solution (50 mM, pH 7) in which the oxygen was purged by nitrogen gas sparging, with PBS (50 mM, pH 7) selected for the catholyte. Air was constantly supplied to the cathode chamber during MFC operation in order to provide a sufficient supply of electron acceptors (oxygen). Both chambers were stirred using a magnetic bar, at a speed of 300 rpm.

### 2.3. Analyses and calculations

The data for the voltage generated in the MFC and each electrode potential was collected in real time using a multimeter (Keithley Instruments, USA). The current ( $I$ ) was derived from the measured voltage ( $U$ ) [24]. A pH meter (Orion 3 star, Thermo Scientific, USA) was utilized to obtain the pH values of the anode and cathode chambers at the start and end of batch operation. The current ( $I$ ) and Coulombic efficiency (CE) were determined using the equations  $I = U/R_e$  and  $CE (\%) = \int I dt / FbMv \times 100$ , respectively, where  $R_e$  is the applied external resistance,  $F$  is Faraday's constant,  $b$  is the mole of electron theoretically harvested from the substrate, and  $v$  is the solution volume.

The power generation capacity and internal resistance evaluations of the MFC were recorded using a potentiostat having a two-electrode set up. Before these two evaluation tests, the MFC reactor fed with a sufficient substrate was operated under open circuit conditions for 6 h in order to achieve a steady state. To assess the MFC power generation capacity, polarization curves were plotted in liner sweep voltammetry mode at a scan rate of 0.1 mV/s. The PD was then determined from the obtained polarization curves [15]. To examine the internal resistance of the MFC, impedance spectra were measured over a frequency range of  $10^{-1}$  to  $10^5$  Hz. The obtained impedance spectra were simulated using frequency response analyzer software (Autolab, EcoChemie, The Netherlands) in order to further examine the tendencies of the internal resistance.

## 3. Results and discussion

### 3.1. Morphologies of membranes

Fig. 3 presents the SEM images of a PEM (Nafion 117) and two ceramic filtration membranes (Anodisc 13 and Sterlitech 15), in which the three membranes clearly exhibit different cross-sectional morphologies. According to the cross-sectional observation of each membrane, Nafion 117, which consists of a hydrophobic fluorocarbon backbone and hydrophilic sulfonate groups, had a single nonporous dense layer, and a measured thickness of about 178  $\mu\text{m}$ . However, the Anodisc 13 ceramic filtration membrane (average pore size: 0.1  $\mu\text{m}$ ), which is comprised of aluminum oxide, had a single-layered highly porous structure having a near unity tortuosity and an observed thickness of 63.5  $\mu\text{m}$ . The second ceramic filtration membrane (Sterlitech 15), which had a molecular weight cut-off of 15 kDa, displayed an asymmetric structure; this membrane consists of a zirconium oxide surface and alumina-titanium oxide-zirconium oxide support layer [25,26]. The pore network of Sterlitech 15 was highly tortuous compared to Anodisc 13, and had a thickness of approximately 2.66 mm.

### 3.2. Membrane resistance

Impedance spectra analyses of electrochemical cells having different types of separators were carried out to determine the membrane electrical resistances, with impedance spectra of an electrochemical cell containing a 0.5 M NaCl solution with no membrane used as a control. Fig. 4 presents the impedance magnitude over frequency for Nafion 117, Anodisc 13, and Sterlitech 15. Constant impedance values from a high frequency regime to a low frequency regime were observed in all impedance spectroscopy measurements, implying that each electrochemical cell is a homogeneous system [27]. When the electrochemical cell had only a 0.5 M NaCl solution with no membrane, the impedance magnitude was 19.2  $\Omega$ . Electrochemical cells having Nafion 117 and Anodisc 13 membranes had slightly higher impedance magnitudes of 20.9 and 22.2  $\Omega$ , respectively, whereas the electrochemical cell having a Sterlitech 15 membrane displayed a much higher impedance magnitude of 245.2  $\Omega$ .

In general, the impedance responses for the high frequency ranges were derived from the electrolyte and membrane [28]. Thus, the electrical resistance value of each membrane can be obtained. Nafion 117 (1.7  $\Omega$ ) and Anodisc 13 (3.0  $\Omega$ ) exhibited

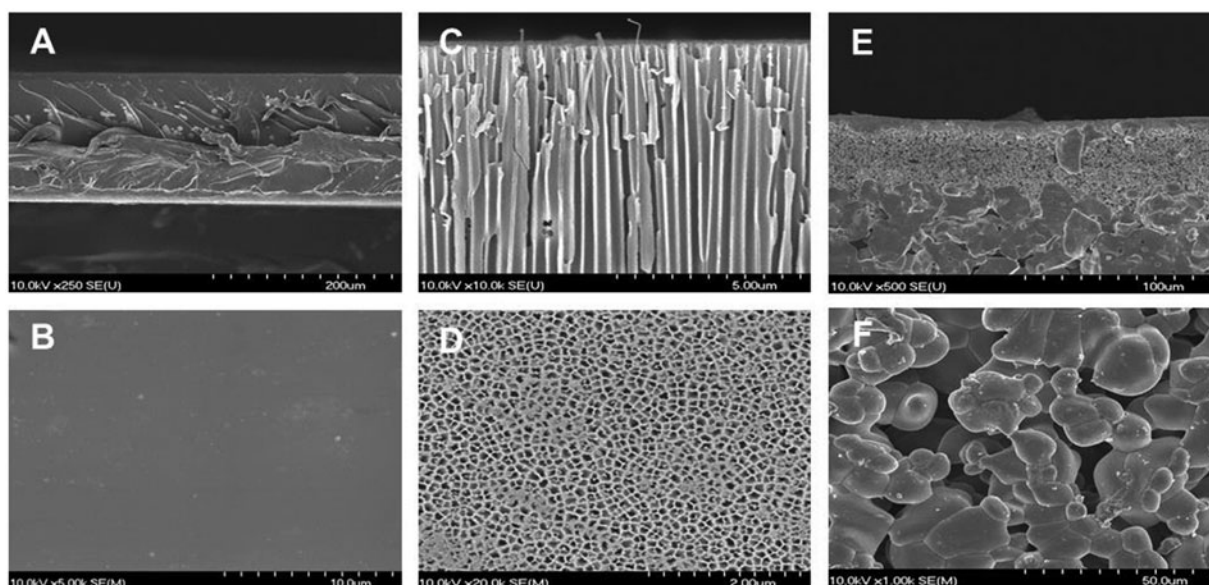


Fig. 3. SEM images of three membranes: cross-sections of (A) Nafion 117, (B) Anodisc 13, and (C) Sterlitech 15; top surfaces of (D) Nafion 117, (E) Anodisc 13, and (F) Sterlitech 15.

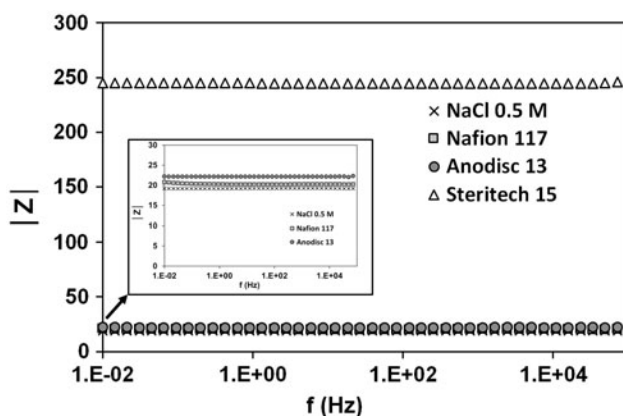


Fig. 4. Impedance of the two-chambered electrochemical cell having no membrane, Nafion 117, Anodisc 13, or Sterlitech 15 as a function of frequency.

comparably lower membrane resistances. Nafion 117 has a high cation mobility due to its sulfonated group, whereas Anodisc 13 has a very small thickness ( $63.5 \mu\text{m}$ ) with great porosity and low tortuosity due to the well-ordered cylindrical pores. However, the membrane resistance of Sterlitech 15 was  $226.0 \Omega$ , which was attributed to its greater thickness ( $2.66 \text{ mm}$ ), highly tortuous pore structure, and small pore size.

### 3.3. Oxygen and substrate diffusion through membranes

Oxygen diffusion from the cathode chamber to the anode chamber and substrate diffusion from the anode chamber to the cathode chamber across a separator in MFCs are the main contributors to performance degradation in MFCs. Oxygen diffusion into the anode chamber through a separator reduces the electricity generation performance for MFCs; the viability of EAB can be inhibited by diffused oxygen, as the diffused oxygen can be preferentially utilized as the electron acceptor [2,29]. In addition, unfavorable substrate losses through membranes during MFC operation reduce the CE [30]. Finally, the substrate from the anode chamber can be utilized by aerobic bacteria and subsequently contribute to biofilm formation on the cathode electrode. These conditions all lead to a deterioration in the performance of cathodic catalysts [5]. Therefore, oxygen and substrate (acetate) diffusion through ceramic filtration membranes were evaluated in the abiotic MFC reactor.

Table 1 presents the oxygen and substrate transfer coefficients for the three membranes used in this study, and other separators reported in previous studies. The oxygen mass transfer coefficients ( $K_o$ ) for Nafion 117, Anodisc 13, and Sterlitech 15 were  $3.60 \times 10^{-4}$ ,  $6.30 \times 10^{-4}$ , and  $0.08 \times 10^{-4} \text{ cm/s}$ , respectively. The  $K_o$  for Nafion 117 in this study is higher than previously reported  $K_o$  values;  $K_o$  values for Nafion 117 reported by Kim et al. [23] and Hou et al.

Table 1

Mass transport through membranes: oxygen transport and substrate transport coefficients for each membrane

Membrane type	Oxygen transfer coefficient, $K_o$ ( $\times 10^{-4}$ cm/s)	Substrate (acetate) transfer coefficient, $K_s$ ( $\times 10^{-7}$ cm/s)	Refs.
Nafion 117	3.60	9.50	In this study
Nafion 117	2.05	–	[31]
Nafion 117	1.30	0.43	[23]
Anodisc 13 (0.1 $\mu$ m)	6.30	23.2	In this study
Sterlitech 15 (15 KD)	0.08	1.30	In this study
CMI-7000	0.94	0.14	[23]
AMI-7001	0.94	0.55	[23]
UF (0.5 KD)	0.19	0.09	[23]
UF (1 KD)	0.41	1.60	[23]
UF (3 KD)	0.42	0.27	[23]
UF (5 KD)	2.14	–	[31]
UF (10 KD)	2.24	–	[31]
MF	4.98	–	[31]
J-Cloth	29.0	–	[32]
Glass fiber	0.50	–	[32]

[31] are  $1.30 \times 10^{-4}$  and  $2.05 \times 10^{-4}$  cm/s. Anodisc 13 has a higher  $K_o$  value compared to the other separators, except for J-Cloth; Sterlitech 15 displays the lowest  $K_o$  value.

Similar to the oxygen transfer, the  $K_s$  value for Nafion 117 in this study is much higher than that reported by Kim et al. [23]. In addition, Anodisc 13 was found to have the highest mass transfer coefficient value for the substrate ( $K_s$ ) ( $23.2 \times 10^{-7}$  cm/s). However, Sterlitech 15 has a much lower  $K_s$  value than Anodisc 13. The  $K_s$  for Sterlitech 15 is comparable to the  $K_s$  for a UF membrane (1 KD) reported by Kim et al. [23].

The higher  $K_o$  and  $K_s$  for Anodisc 13 can be explained as being due to its cylindrical microsized pores and small thickness. In contrast to Anodisc 13, the small pore size and large thickness of Sterlitech 15 leads to its low oxygen and substrate transport.

### 3.4. Voltage generation

MFCs equipped with Nafion 117, Anodisc 13, and Sterlitech 15 were operated at an external resistance of 100  $\Omega$  in a batch mode, in order to compare their cell voltage generation (Fig. 5). The respective voltages generated (or current generated) were  $57.3 \pm 3.6$  mV ( $0.57 \pm 0.04$  mA),  $67.7 \pm 1.9$  mV ( $0.68 \pm 0.02$  mA), and  $32.9 \pm 1.8$  mV ( $0.33 \pm 0.02$  mA). The Coulombic efficiencies for Nafion 117, Anodisc 13, and Sterlitech 15 were  $17.8 \pm 4.3$ ,  $26.5 \pm 1.9$ , and  $16.3 \pm 1.5\%$ . Notably, the highest voltage and CE were produced in the

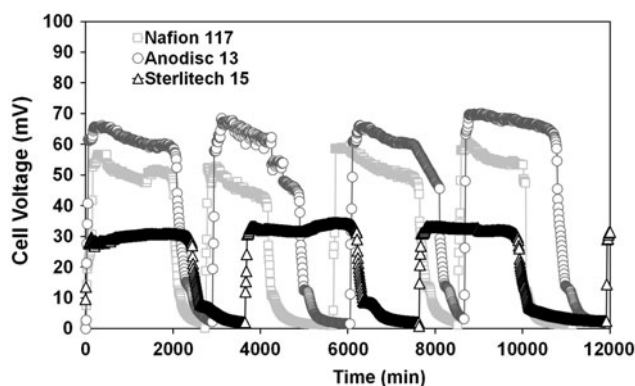


Fig. 5. Voltage generation in MFCs using three membranes: Nafion 117, Anodisc 13, and Sterlitech 15.

MFC having Anodisc 13, although Anodisc 13 showed the highest oxygen and substrate diffusion rate in the oxygen and substrate diffusion tests. The most likely explanation is that the microsized cylindrical pores in Anodisc 13 facilitated a high proton transport. Less pH variation for Anodisc 13, compared to Nafion 117 and Sterlitech 15, supports this explanation (Fig. 6). On the other hand, Sterlitech 15 exhibited the lowest voltage generation, likely due to the following reasons: (1) the approximately 100 times higher electrical membrane resistance than for the other membranes, and (2) the retardation of proton transport due to its compact pore size, larger thickness, and highly tortuous pore structure.

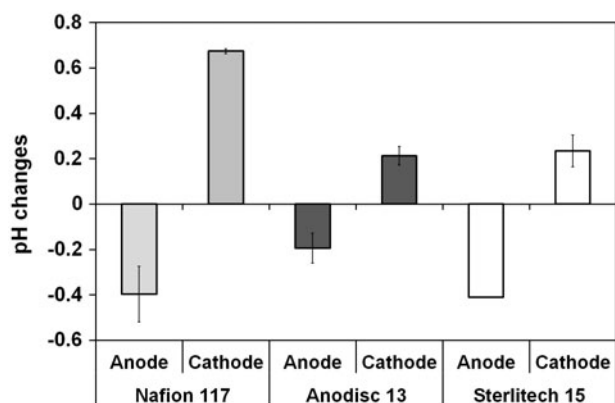


Fig. 6. pH variations in MFCs having Nafion 117, Anodisc 13, and Sterlitech 15 at the end of a single-batch cycle.

### 3.5. Comparison of PD and internal resistance

To further understand factors affecting electricity generation in MFCs having ceramic filtration membranes, the internal resistances of these MFCs were explored using impedance spectroscopy. The data obtained from the impedance spectra analyses are displayed in a Nyquist plot in Fig. 7(b). The total internal resistance values and each component of the internal

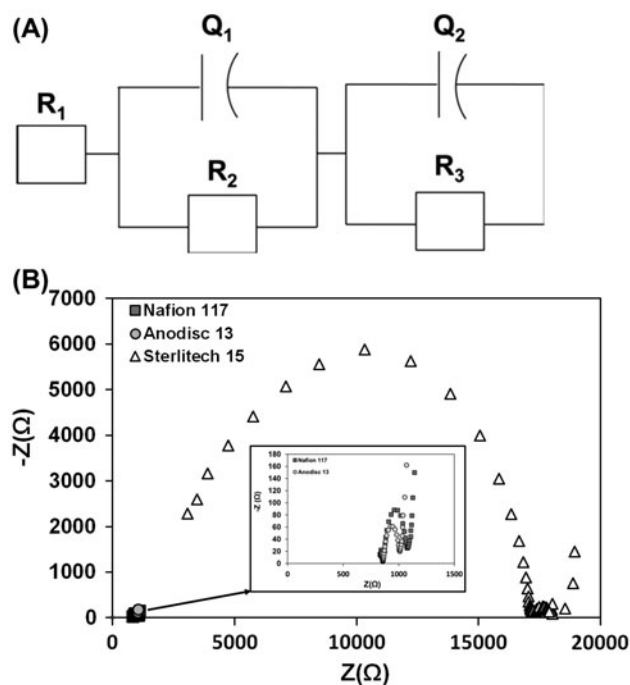


Fig. 7. (A) Equivalent circuit and (B) Nyquist plot obtained from the impedance spectra measurements of the MFC.

resistance of the MFC were obtained by fitting the impedance data to a typical equivalent circuit that describes the electrochemical reaction components in an MFC (Fig. 7(a)) [33,34]. The equivalent circuit is comprised of one ohmic resistance component ( $R_1$ ), which originates from the anolyte, the catholyte, a membrane, and two sets of parallel charge transfer resistance/constant phase elements ( $R_2/Q_1$  and  $R_3/Q_1$ ), which are related to the anodic and cathodic activation energy and the electrical double layer formed between the electrode and electrolyte [33–35].

Similar ohmic resistance values were obtained in MFCs having Nafion 117 (728.0  $\Omega$ ) and Anodisc 13 (733.0  $\Omega$ ), with a higher ohmic resistance of 894.0  $\Omega$  observed for Sterlitech 15. In all MFC tests, identical anolytes and catholytes were utilized; the different MFC ohmic resistances were thus attributed to the installed membrane, which is in agreement with the results of the electrical membrane resistance measurements. Unlike the ohmic resistance, however, Anodisc 13 exhibited a lower charge transfer resistance (252.7  $\Omega$ ) than Nafion 117 (323.8  $\Omega$ ), with Sterlitech 15 having an extremely higher charge transfer resistance (19,790.0  $\Omega$ ).

Previous studies also found that MFCs having microfiltration polymer membranes had lower internal resistances [31,36], as the charge transfer resistance is closely related to electron transfer steps in MFCs [13]. For electrical neutrality, as electrons move from the anode chamber to the cathode chamber, the same electrochemically equivalent positive ions should transfer (theoretically, protons for the reduction of oxygen); thus, electron and ion transfers can mutually affect each other. From this relationship, we can infer that the reason for the lower charge transfer resistance with Anodisc 13 was the greater transport of ionic species—including protons—through Anodisc 13 due to its small thickness, large pore size, and highly porous and non-tortuous pore structure. On the other hand, the excessively large charge transfer resistance for Sterlitech 15 is likely due to inferior ion transport arising from its larger thickness, relatively small pore size (UF: 5 KD), and highly tortuous pore structure.

Finally, polarization tests were performed to examine the power generation capacity during the operation of MFCs having different membranes (Fig. 8). The highest maximum PD of 0.12 W/m<sup>2</sup> was obtained in the MFC having an Anodisc 13 membrane, with a slightly lower maximum PD of 0.10 W/m<sup>2</sup> achieved with Nafion 117; Nafion 117 has a higher charge transfer resistance than Anodisc 13. Sterlitech 15 exhibited a substantially lower maximum PD of 0.01 W/m<sup>2</sup> due to its enormously large ohmic and charge transfer resistances.

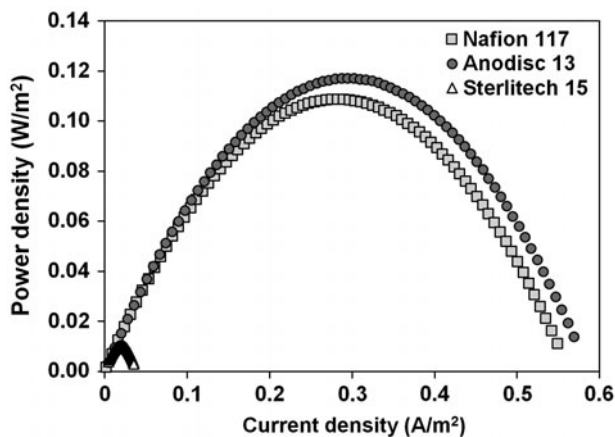


Fig. 8. PD curves of MFCs having three membranes: Nafion 117, Anodisc 13, and Sterlitech 15.

#### 4. Conclusions

We demonstrated the feasibility of using ceramic filtration membranes (Anodisc 13 and Sterlitech 15) as separators in MFCs. Although higher oxygen and substrate transfer coefficients were observed across Anodisc 13 in the mass transport tests, during MFC operation, MFCs having an Anodisc 13 membrane generated more electricity compared to Nafion 117; because its smaller membrane thickness and cylindrical micro-sized pores led to a higher proton transport and lower charge and diffusion resistances. In contrast, Sterlitech 15 exhibited poor electrical energy performance due to its greater thickness, high tortuosity, and tighter pores. In conclusion, for ceramic filtration membranes to be applied in MFCs, they should have a small thickness and low resistance. To identify the optimum thickness and pore size of ceramic filtration membranes, however, further investigations are needed.

#### Acknowledgements

This research was supported by a grant (code 151FIP-B088091-02) from the Industrial Facilities and Infrastructure Research Program funded by the Ministry of Land, Infrastructure and Transport of the Korean government, and in part by the National Research Foundation of Korea (NRF) grant funded by the Korea government (MSIP) (No. 2015R1C1A1A01054039).

#### References

- [1] I.S. Kim, K.-J. Chae, M.J. Choi, W. Verstraete, Microbial fuel cells: Recent advances, bacterial communities and application beyond electricity generation, *Environ. Eng. Res.* 13 (2008) 51–65.
- [2] K.J. Chae, M. Choi, F.F. Ajayi, W. Park, I.S. Chang, I.S. Kim, Mass transport through a proton exchange membrane (Nafion) in microbial fuel cells, *Energy Fuels* 22 (2008) 169–176.
- [3] S.M. Daud, B.H. Kim, M. Ghasemi, W.R.W. Daud, Separators used in microbial electrochemical technologies: Current status and future prospects, *Bioresour. Technol.* 195 (2015) 170–179.
- [4] B.R. Dhar, H.-S. Lee, Membranes for bioelectrochemical systems: Challenges and research advances, *Environ. Technol.* 34 (2013) 1751–1764.
- [5] K.-Y. Kim, K.-J. Chae, M.-J. Choi, E.-T. Yang, M.H. Hwang, I.S. Kim, High-quality effluent and electricity production from non-CEM based flow-through type microbial fuel cell, *Chem. Eng. J.* 218 (2013) 19–23.
- [6] W.W. Li, G.P. Sheng, X.W. Liu, H.Q. Yu, Recent advances in the separators for microbial fuel cells, *Bioresour. Technol.* 102 (2011) 244–252.
- [7] R.A. Rozendal, H.V.M. Hamelers, C.J.N. Buisman, Effects of membrane cation transport on pH and microbial fuel cell performance, *Environ. Sci. Technol.* 40 (2006) 5206–5211.
- [8] M.-J. Choi, K.-J. Chae, F.F. Ajayi, K.-Y. Kim, H.-W. Yu, C.-W. Kim, I.S. Kim, Effects of biofouling on ion transport through cation exchange membranes and microbial fuel cell performance, *Bioresour. Technol.* 102 (2011) 298–303.
- [9] J. Xu, G.P. Sheng, H.W. Luo, W.W. Li, L.F. Wang, H.Q. Yu, Fouling of proton exchange membrane (PEM) deteriorates the performance of microbial fuel cell, *Water Res.* 46 (2012) 1817–1824.
- [10] A. Ter Heijne, H.V.M. Hamelers, V. De Wilde, R.A. Rozendal, C.J.N. Buisman, A bipolar membrane combined with ferric iron reduction as an efficient cathode system in microbial fuel cells, *Environ. Sci. Technol.* 40 (2006) 5200–5205.
- [11] L. Dammak, C. Larchet, D. Grande, Ageing of ion-exchange membranes in oxidant solutions, *Sep. Purif. Technol.* 69 (2009) 43–47.
- [12] R.A. Rozendal, H.V.M. Hamelers, K. Rabaey, J. Keller, C.J.N. Buisman, Towards practical implementation of bioelectrochemical wastewater treatment, *Trends Biotechnol.* 26 (2008) 450–459.
- [13] K.-Y. Kim, E. Yang, M.-Y. Lee, K.-J. Chae, C.-M. Kim, I.S. Kim, Polydopamine coating effects on ultrafiltration membrane to enhance power density and mitigate biofouling of ultrafiltration microbial fuel cells (UF-MFCs), *Water Res.* 54 (2014) 62–68.
- [14] Z. Ge, Q. Ping, L. Xiao, Z. He, Reducing effluent discharge and recovering bioenergy in an osmotic microbial fuel cell treating domestic wastewater, *Desalination* 312 (2013) 52–59.
- [15] C.M. Werner, B.E. Logan, P.E. Saikaly, G.L. Amy, Wastewater treatment, energy recovery and desalination using a forward osmosis membrane in an air-cathode microbial osmotic fuel cell, *J. Membr. Sci.* 428 (2013) 116–122.
- [16] F. Zhang, K.S. Brastad, Z. He, Integrating forward osmosis into microbial fuel cells for wastewater treatment, water extraction and bioelectricity generation, *Environ. Sci. Technol.* 45 (2011) 6690–6696.



- [17] J. Winfield, L.D. Chambers, J. Rossiter, I. Ieropoulos, Comparing the short and long term stability of biodegradable, ceramic and cation exchange membranes in microbial fuel cells, *Bioresour. Technol.* 148 (2013) 480–486.
- [18] M. Behera, P.S. Jana, M.M. Ghangrekar, Performance evaluation of low cost microbial fuel cell fabricated using earthen pot with biotic and abiotic cathode, *Bioresour. Technol.* 101 (2010) 1183–1189.
- [19] Z. Ge, Z. He, Effects of draw solutions and membrane conditions on electricity generation and water flux in osmotic microbial fuel cells, *Bioresour. Technol.* 109 (2012) 70–76.
- [20] G. Pasternak, J. Greenman, I. Ieropoulos, Comprehensive study on ceramic filtration membranes for low-cost microbial fuel cells, *ChemSusChem* 9 (2015) 88–96.
- [21] J. Winfield, J. Greenman, D. Huson, I. Ieropoulos, Comparing terracotta and earthenware for multiple functionalities in microbial fuel cells, *Bioprocess. Biosyst. Eng.* 36 (2013) 1913–1921.
- [22] R. Ciora, P.K. Liu, Ceramic membranes for environmental related applications, *Fluid/Particle Sep. J.* 15 (2003) 51–60.
- [23] J.R. Kim, S. Cheng, S.E. Oh, B.E. Logan, Power generation using different cation, anion, and ultrafiltration membranes in microbial fuel cells, *Environ. Sci. Technol.* 41 (2007) 1004–1009.
- [24] S. Oh, B. Min, B.E. Logan, Cathode performance as a factor in electricity generation in microbial fuel cells, *Environ. Sci. Technol.* 38 (2004) 4900–4904.
- [25] G.D. Bothun, Q. Ni, S. Ilias, Solvent-dependent permeability in asymmetric ceramic membranes with tortuous or non-tortuous mesopores, *J. Membr. Sci.* 325 (2008) 982–988.
- [26] S.-J. Lee, J.-H. Kim, Differential natural organic matter fouling of ceramic versus polymeric ultrafiltration membranes, *Water Res.* 48 (2014) 43–51.
- [27] Y. Gao, W. Li, W.C. Lay, H.G. Coster, A.G. Fane, C.Y. Tang, Characterization of forward osmosis membranes by electrochemical impedance spectroscopy, *Desalination* 312 (2013) 45–51.
- [28] J.-S. Park, J.-H. Choi, J.-J. Woo, S.-H. Moon, An electrical impedance spectroscopic (EIS) study on transport characteristics of ion-exchange membrane systems, *J. Colloid Interface Sci.* 300 (2006) 655–662.
- [29] K. Kang, J. Jang, T. Pham, H. Moon, I. Chang, B. Kim, A microbial fuel cell with improved cathode reaction as a low biochemical oxygen demand sensor, *Biotechnol. Lett.* 25 (2003) 1357–1361.
- [30] Y. Zuo, S. Cheng, B.E. Logan, Ion exchange membrane cathodes for scalable microbial fuel cells, *Environ. Sci. Technol.* 42 (2008) 6967–6972.
- [31] B. Hou, J. Sun, Y.-Y. Hu, Simultaneous Congo red decolorization and electricity generation in air-cathode single-chamber microbial fuel cell with different microfiltration, ultrafiltration and proton exchange membranes, *Bioresour. Technol.* 102 (2011) 4433–4438.
- [32] X. Zhang, S. Cheng, X. Wang, X. Huang, B.E. Logan, Separator characteristics for increasing performance of microbial fuel cells, *Environ. Sci. Technol.* 43 (2009) 8456–8461.
- [33] Z. He, F. Mansfeld, Exploring the use of electrochemical impedance spectroscopy (EIS) in microbial fuel cell studies, *Energy Environ. Sci.* 2 (2009) 215–219.
- [34] Z. He, N. Wagner, S.D. Minteer, L.T. Angenent, An upflow microbial fuel cell with an interior cathode: Assessment of the internal resistance by impedance spectroscopy, *Environ. Sci. Technol.* 40 (2006) 5212–5217.
- [35] E. Yang, M.-J. Choi, K.-Y. Kim, K.-J. Chae, I.S. Kim, Effect of initial salt concentrations on cell performance and distribution of internal resistance in microbial desalination cells, *Environ. Technol.* 36 (2014) 852–860.
- [36] J. Sun, Y. Hu, Z. Bi, Y. Cao, Improved performance of air-cathode single-chamber microbial fuel cell for wastewater treatment using microfiltration membranes and multiple sludge inoculation, *J. Power Sources* 187 (2009) 471–479.